Transcriptome Analysis of Drought Stress and Rehydration in the *Trachycarpus fortunei* Seedling Stage

Xiao Feng
Guizhou University
Zhao Yang (zhy737@126.com)
Guizhou University https://orcid.org/0000-0002-2558-9216
Wang Xiu-Rong
Guizhou University

Research article

Keywords: Trachycarpus fortunei, transcriptome, drought stress, rehydration, WGCNA

Posted Date: February 26th, 2020

DOI: https://doi.org/10.21203/rs.2.24473/v1

Abstract

Background: *Trachycarpus fortunei* has broad economic benefits and excellent drought resistance; however, its drought response, adaptation, and recovery processes remain unclear. In this study, the response, tolerance, and recovery processes of *T. fortunei* leaves and roots under drought stress were determined by Illumina sequencing.

Results: Under drought stress, *T. fortunei* reduced its light-capturing ability and composition of its photosynthetic apparatus, thereby reducing photosynthesis to prevent photo-induced chloroplast reactive oxygen damage during dehydration. The phenylpropanoid biosynthesis process in the roots was contained and ABA induced the accumulation of intracellular osmoprotectants, as well as *DHNs*, *LEA, Annexin D2*, *NAC*, and other genes, which may play important roles in protecting the cell membrane's permeability in *T. fortunei* root tissues. During the rehydration phase, fatty acid biosynthesis in *T. fortunei* roots was repressed. Weighted correlation network analysis (WGCNA) screened modules that were positively or negatively correlated with physiological traits. The Real-time quantitative PCR (RT-qPCR) results indicated the reliability of the transcriptomic data.

Conclusions: These findings provide valuable information for identifying important components in the *T. fortunei* drought signaling network and enhances our understanding of the molecular mechanisms by which *T. fortunei* responds to drought stress.

Background

Trachycarpus fortunei (Hook.) H. Wendl. (Fam.: Palmae; Gen.: Trachycarpus) is an evergreen tree that is widely distributed. It is an important economic and landscaping plant. T. fortunei possesses strong drought resistance and rapid recovery ability after rehydration [1]. Currently, the response mechanism of T. fortunei to drought stress remains unclear. Under drought stress, leaf stomata are closed, cells undergo osmotic adjustments, and the amount of free sugar and free amino acids increase, especially proline [2–3]. When drought persists, proteins may lose their activity or denature, producing excessive reactive oxygen species (ROS), thereby promoting oxidative kinase activities in leaf cells and inhibiting photosynthesis, leading to metabolic dysfunction and the destruction of cellular structures [4–6]. Various drought-induced signaling pathways regulated by abscisic acid (ABA) are activated, and ROS are rapidly cleared [7]. As the degree of drought increases, plants are subjected to plastic damage, growth retardation, and even death.

In this study, the seedlings of T. fortunei whole siblings were used as the experimental materials to simulate the natural drought stress process, and the expression profiles of drought resistance-related genes were obtained. The phenotype and physiological indexes were combined to explore the responses and recovery mechanisms of T. fortunei seedlings to drought stress. The findings of this study serve as an important basis for T. fortunei drought resistance breeding and cultivation.

Results

Plant-related physiological and biochemical indicators

During the experiment, AMC decreased continuously from 0 to 15 d (Fig. 1B). Leaves entered the folded state after 9 d (Fig. 1A). After 9 d, the POD content reached its maximum value (Fig. 1G), while SOD was at its lowest value (Fig. 1H). After 12 d, the leaves were folded and curled, leaf area decreased, and the MDA content in the roots increased to its maximum value (Fig. 1D), the Pro activity in the leaves reached its maximum value (Fig. 1H), and the MDA content in the leaves reached its maximum value, but was delayed compared to the roots (Fig. 1E). After 15 d, SOD reached its peak value (Fig. 1G), and Rv (Fig. 1I) and area (Fig. 1C) decreased to their lowest values. After 12 and 15 d, samples clustered into one group (Fig. 1K). After rehydration, most T. fortunei gradually stretched at Re0.5d. Each indicator showed a correlation with the positive/negative modes of stress (Fig. 1L). The PCA results revealed that Re6d and 0 d were closer and coercion was lifted (Fig. 1H).

Data quality control, splicing, comparison, expression quantification, and differential analysis

The raw data of each sample (Q30) ranged from 96.88–97.57%. The effective data ranged from 6.98–7.18 G. The average GC content was 47.94%. The four base content distribution of each sample was relatively uniform. A total of 66,270 unigenes were spliced with a total length of 55,575,529 bp and an average length of 840 bp. In total, 43,238 (65.25%) unigenes were annotated in the NCBI NR database, while 30,054 (45.35%) unigenes were annotated in the Swiss-Prot database. A total of 51,381 CDS sequences were predicted, of which, 43,373 were predicted by the database comparison method and 8,008 were predicted by ESTScan. Among them, 8.08% of the unigene TFs were compared to oil palm (Elaeis guineensis) and 5.95% were compared to apples (Malus domestica); a total of 15,696 unigene annotations were identified in the TF database and were distributed across 58 families. The raw data were stored in the NCBI/SRA database (BioProject accession No.: PRJNA598974).

The distance clustering heatmap between the samples revealed that the samples were reproducible and the leaf and root tissues were distinct (Fig. 2A). PCA revealed that the repeatability was better among groups and the cumulative contribution rate was high (Fig. 2B). After screening for DEGs, compared to 0d_L (Fig. 2C), the DEGs of the corresponding parts of each stage included 4,791 (9 d), 9,108 (15 d), 5,480 (Re0.5d), and 3,211 (Re1d) DEGs. Compared to 0d_R (Fig. 2D), the DEGs of the corresponding parts of each stage included 7,995 (9 d), 8,556 (15 d), 4,968 (Re0.5d), and 6,204 (Re1d) DEGs. After 15 d, the number of DEGs reached its peak value compared to 0 d. The five differential combinations between the L and R sites had a total difference of 11,510 DEGs (Fig. 2E), which were associated with tissue specificity.

Functional enrichment analysis of DEGs

The GO similarity enrichment (BP category) revealed that the leaf responses to hormones were active in the L1 group (Fig. 2H). In the L2 group, photosynthesis (ko00195), photosynthesis-antenna proteins (ko00196), and porphyrin and chlorophyll metabolism (ko00860) were the most enriched terms (Fig. 2I). Most of the DEGs in the pathway were downregulated in 15d_L. The light-harvesting complex I chlorophyll a/b binding protein 1–5 (Lcha1-5) and Lhcb1-7 were lowered in 15d_L.

The biosynthesis of metabolites in the roots was enriched in the R2 group (Fig. 2I). In the R2 group, the most significantly enriched pathway included phenylpropanoid biosynthesis (ko00940), and most of the ko00940 DEGs were downregulated in 15d_R. In the R1, R3, and R4 groups, fatty acid biosynthesis (ko00061) and fatty acid metabolism (ko01212) were enriched.

The recovery of plant phenotypes was rapidly developed after rehydration. In the 15d_L/Re0.5d_L group, photosynthesis-related genes were activated, and Lca1-5 and Lcb2-6 were upregulated in Re0.5d_L. In the R3 group, fatty acid biosynthesis (ko00061)-related DEGs were all downregulated in Re0.5d.

The STEM analysis revealed that there were 16 significantly different modules in the leaf group (Fig. 3A), profile 23 (0.0, 0.0, -1.0, 1.0, 1.0) (Fig. 3D), and profile 10 (0, -1, -2, -1, 0) (Fig. 3C), which all dropped to their lowest values after 15 d. In profile10, photosynthesis (ko00195), photosynthesis-antenna proteins (ko00196), carbon fixation in photo, and synthetic organisms (ko00710) were enriched. Profile43 (0.0, 1.0, 3.0, 3.0, 2.0)-related gene expression increased to its maximum value after 15 d (Fig. 3G). Starch and sucrose metabolism (ko00500) and diterpenoid biosynthesis (ko00904) were enriched in Profile43. Profile25 (0.0, 0.0, 0.0, -1.0, 1.0) and profile 36 (0.0, 1.0, 1.0, -1.0, 1.0)-related gene expression were reduced to their lowest values in Re0.5d (Fig. 3E, F). Arachidonic acid metabolism (ko00590) and linoleic acid metabolism (ko00591) were enriched in profile25. Fatty acid biosynthesis (ko00061) and fatty acid elongation (ko00062) were enriched in profile36.

There were 15 significant differences in the root group (Fig. 3B). Profile10 (0.0, -1.0, -2.0, -1.0, 0.0)-related gene expression reached its lowest value after 15 d (Fig. 3H). Phenylpropanoid biosynthesis (ko00940) and glycosaminoglycan degradation (ko00531) were enriched in Profile10. Profile42 (0.0, 1.0, 3.0, 1.0, 2.0)-related gene expression peaked after 15 d (Fig. 3K), at which point, linoleic acid metabolism (ko00591), cutin, suberine, and wax biosynthesis (ko00073), and sulfur metabolism (ko00920) were enriched. In Profile25 (0.0, 0.0, 0.0, -1.0, 1.0), fatty acid biosynthesis (ko00061) was enriched (Fig. 3I). Profile36 (0.0, 1.0, 1.0, -1.0, 1.0)-related gene expression reached its lowest values in Re0.5d (Fig. 3J). Starch and sucrose metabolism (ko00500) and galactose metabolism (ko00052) were also enriched in Profile36.

Weighted correlation network analysis

The Weighted correlation network analysis (WGCNA) revealed that the leaves divided into 14 modules and the roots divided into 11 modules. In the leaf co-expression analysis network (Fig. 4A), the lightcyan1 and dark turquoise modules were significantly positively correlated with multiple traits, the black module was significantly negatively correlated with multiple traits, and the brown4 module was correlated with rehydration stress expression after 15 d in Re0.5d (Fig. 4C). The GO enrichment analysis (CC category) revealed that it was associated with thylakoid (GO: 0009579) and chloroplast thylakoid (GO: 0009534). The brown module was significantly positively correlated with area (Correlation coefficient = 0.63, P = 0.01). Additionally, the GO enrichment analysis (CC category) indicated that chloroplast thylakoid and plastid thylakoid (GO: 0031974) were enriched. The darkorange2 module and AMC were significantly positively correlated(Correlation coefficient = 0.8, P = 4e-04), protein heterodimerization activity (GO:0046982) was enriched (MF category).

In the root co-expression analysis network (Fig. 4B), the black module was significantly negatively correlated with area (Correlation coefficient= -0.99, P = 2e-13). Response to water (GO: 0009415), response to cold (GO: 0009409), and response to salt stress (GO: 0009651) (BP category) were enriched. DHNs COR410-like (TRINITY_DN51483_c1_g1_i2), LEA14 (TRINITY_DN41505_c0_g2_i2), NAC 47 (TRINITY_DN48903_c0_g2_i1), and Annexin D2 (TRINITY_DN46177_c1_g1_i1) aggregated in response to water (GO: 0009415). The light green module was significantly positively correlated with area (Correlation coefficient = 0.96, P = 2e-08). Protein heterodimerization activity (GO:0046982), water transmembrane transporter activity (GO: 0005372), and water channel activity (GO:0015250) (CC category) were enriched.

Real-time quantitative PCR results

The RT-qPCR results revealed that Annexin D2 (Fig. 5B), DHNs COR410 (Fig. 5D), and NAC 47 (Fig. 5F) were upregulated after 15 d. Log2 $^{(\text{Fold change})}$ and log2 $^{(2-\Delta\Delta Ct)}$ were subjected to linear correlation analyses (Fig. 5J). Results revealed a positive correlation (0.79) with the RNA-Seq results (R^2 = 0.65). Thus, the RT-qPCR and RNA-Seq data were relatively consistent.

Discussion

Drought is one of the main abiotic stressors affecting plant growth and development. After entering the drought state, T. fortunei leaves fold, root activity continuously decreases, Pro activity continuously increases, and the genes related to photosynthesis (ko00195) and photosynthesis-antenna proteins (ko00196) are continuously downregulated (0, -1, -2, -1, 0). Under drought stress, the light absorption of antenna proteins decreases, electron transport rates of PSII and PSI decreases, photosynthetic electron transport chain decreases overall, ROS accumulation increases, photosynthetic pigments are destroyed, RAC activity decreases, and chlorophyll content decreases [8–13]. Resuscitation plants are able to survive 95% of their cell water loss, one tolerance mechanism is to reversibly shut down photosynthesis, for example, in Xerophyta humilis, psbR, psbA, and psbP were downregulated during dehydration, and complex water regulation expression trends were exhibited [14–15]. In this study, under drought stress, the expression of chlorophyll a-b binding proteins decreased and the synthesis of photosynthesis-related factors decreased. After rehydration, RAC and other photosynthetic-related genes were activated and recovered to a relatively consistent level after 0 d in Re1d. Gene expression of the thylakoid-associated cellular components proliferated after rehydration (Fig. 4C, brown4). T. fortunei Psb O, Psb P, Psb Q, Psb R, and other PSII subunits were downregulated under drought stress and gradually increased after rehydration. T. fortunei also reduced its light-trapping ability and the composition of the photosynthetic apparatus, thereby reducing photosynthesis and increasing drought resistance by leaf folding to prevent light-induced chloroplast ROS damage due to dehydration.

Plant roots may induce specific stress responses to cope with the early perception of soil water loss [16]. In the R2 group, phenylpropanoid biosynthesis (ko00940) was curbed, most of the DEGs (48/53) were downregulated in 15d_R, and some genes (27) of profile10 (0.0, -1.0, -2.0, -1.0, 0.0) were expressed. Protein phosphorylation and dephosphorylation are important signaling events that lead to drought tolerance [17]. PP2C belongs to a group of phosphatases involved in ABA signaling and is a negative regulator [18]. Both PP2C-related DEGs the in L2 and R2 groups were upregulated after 15 d. In order to absorb water and survive under drought stress, permeants (various organic solutes) accumulated in the cytoplasm and chloroplasts for osmotic adjustment [19]. ABA can induce the accumulation of intracellular osmoprotectants, such as the LEA post-embryonic protein, chaperone proteins, carbohydrates, and Pro, which may be critical for survival under drought stress [20]. The relationship between water transmembrane transporter activity (GO: 0005372) and water channel activity (GO:0015250) was positively correlated with area (Fig. 4D, lightgreen), the black module was significantly negatively correlated (Fig. 4D), and the expression of DHNs was generally regulated and induced by ABA, which can reduce root water conductivity [21–23]. LEA proteins bind to a large number of water molecules and maintain normal metabolism in cells [24]. In a previous study, rice OsANN3 was found to mediate $Ca2^{+}$ influx by binding to phospholipids, and overexpression significantly increased drought stress survival [25]. As drought persisted, phenylpropanoid biosynthesis in the roots was suppressed, ABA induced the accumulation of intracellular osmoprotectants, and the DHNs, LEA, Annexin D2, NAC, and other genes were expressed, possibly to protect cell membrane permeability in T. fortunei root tissues.

Resilience is an important physiological feature of drought-tolerant genotypes. The ability to preserve tissue health, integrity, and avoid aging is vitally important. Restorative plants may have pathways that inhibit drought-related senescence [26–28]. The biosynthesis of palmitic (C16:0), linoleic (C18:2), linolenic (C18:3) and stearic acid (C18:0) increased 18, 12, 20, and 8-fold during dehydration in Pleopeltis polypodioide, rehydration lowered levels of peroxides, the activity of glutathione-oxidizing enzymes, and fatty acids [29]. After T. fortunei rehydrated for 12 h, the leaves gradually recovered from the fully folded state. In profile36 (0.0, 1.0, 1.0, -1.0, 1.0), fatty acid biosynthesis (ko00061) (TRINITY_DN53033_c0_g1_i1; TRINITY_DN67658_c0_g1_i1) was enriched in the leaves. Meanwhile, in root profile25 (0.0, 0.0, 0.0, -1.0, 1.0) (Fig. 3B), the fatty acid biosynthesis (ko00061) (TRINITY_DN48458_c0_g1_i1; TRINITY_DN52213_c0_g1_i2; TRINITY_DN53033_c0_g1_i1) pathway was simultaneously enriched. The transcripts of fatty acid biosynthesis (TRINITY_DN53033_c0_g1_i1; TRINITY_DN67658_c0_g1_i1) were annotated as ACCase subunit alpha (acetyl-coenzyme A carboxylase carboxyl transferase subunit alpha, chloroplastic), whose transcripts (TRINITY_DN52213_c0_g1_i2) encoded stearoyl-ACP desaturase (SAD). ACCase is a key, rate-limiting enzyme involved in fatty acid biosynthesis that catalyzes the carboxylation of acetyl-CoA to form malonyl-CoA, providing a substrate for the synthesis of fatty acids and many secondary metabolites [30]. Fatty acid is the main component of cell and organelle membrane lipids. The regulation of membrane lipid contents and compositions is an effective regulation method for adapting to environmental stress under drought conditions, as well as a positive regulation mechanism during recovery after rehydration [31]. In the R3 group, fatty acid biosynthesis (ko00061)-related DEGs were downregulated in Re0.5d and some genes in profile25 (0.0, 0.0, 0.0, -1.0, 1.0) were expressed in the roots. Additionally, β-CT reached its lowest expression level in Re0.5d. This indicated that fatty acid biosynthesis in T. fortunei roots is repressed during the rehydration phase after extreme drought.

Conclusion

Under drought stress, *T. fortunei* reduces its light-trapping ability and the composition of the photosynthetic apparatus, thereby reducing photosynthesis and increasing drought resistance by leaf folding to prevent light-induced chloroplast ROS damage to dehydration. As drought conditions worsen, phenylpropanoid biosynthesis in the roots is suppressed and ABA induces the accumulation of intracellular osmoprotectants, as well as *DHNs*, *LEA*, *Annexin D2*, *NAC*, and other genes that may protect the cellular membrane's permeability in *T. fortunei* root tissues. Fatty acid biosynthesis in *T. fortunei* roots is also repressed after rehydration.

Methods

Test materials

After the investigation and screening of excellent *T. fortunei* provenances in the early stage, the excellent paternal pollen collected in Guiding, Guizhou province, China, was sexually crossed with the excellent female plants in Huaxi, Guizhou province, China. The whole sibling progeny consisting were obtained (None permissions were necessary to collect such samples, the specie was confirmed to be *T. fortunei* by the Professor Wu Feng and Fan Fuhua (Institute for Forest Resources & Environment of Guizhou, Guizhou University), the voucher specimen is accessible at the Institute for Forest Resources & Environment of Guizhou, Guizhou University (accessions No. TF-001-1). Related experimental research, including the collection of plant materials, complies with institutional, national or international guidelines). The whole sibling progeny consisting of 1.5-year-old seedlings was selected for transplanting (four months) and placed in a greenhouse. The soil type in the pot was humus:yellow soil (1:3). Natural drought stress was simulated and plants were normally irrigated for 3 days before drought treatment. At the beginning of the stress experiment, physiological growth, roots, sample retention, and other indicators were measured. The aluminum box soil drying method was used to determine the soil absolute moisture content (AMC). A leaf area scanner was used to sequence the *T. fortunei* leaf area. Sampling was conducted between 8:00–9:00 AM. After 3 days, sampling and the sampling work were repeated; phenotypic changes were also recorded. Samples were collected every 3 days until the fresh leaves of the seedlings were extremely atrophic. At this point, drought stress concluded and the rehydration experiment was conducted. After 12 hours (Re0.5d), 1 day (Re1d), 3 days (Re3d), and 6 days (Re6d), rehydration and related indicators were measured.

Test methods

Determination of physiological indicators

First, mature leaves were collected using plant physiological and biochemical experimental principles and techniques [32]. The proline (Pro) content was determined by acid ninhydrin colorimetry. Malondialdehyde activity (MDA) was determined using the thiobarbituric acid method. Total superoxide dismutase (SOD) was determined using the nitrogen blue tetrazolium photoreduction method. Peroxidase (POD) activity was determined using the phenol method. *T. fortunei* roots were collected to determine the MDA content and root vitality (Rv) using the TTC method. The experiment included 3 biological and technical replicates.

Transcriptome material collection and library construction

The material selection nodes included 0 d, 9 d, 15 d, Re0.5d, and Re1d, each with three biological replicates. The leaf collection site was unified into mature healthy leaves. Root tips were collected from the roots, washed with distilled water, wrapped in tin foil, and stored in liquid nitrogen. Materials were extracted and purified using the CTAB method. After passing the RNA quality and concentration test (A260/280 = 2.0–2.2; A260/230 = 1.8–2.2; 28S/18S = 1.4–2.7; Rin ≥ 8.0), libraries were constructed. Sequencing was conducted on an Illumina HiSeq X Ten machine and completed by the Shanghai Ouyi Co. (Shanghai, China).

Data processing and analysis

Raw data were quality filtered and reads with adapters or poor-quality sequences were removed. Assembly of the reads was performed using the Trimmomatic tool [33]. Then, sequence alignment of the clean data and assemblage of the transcripts and unigene libraries were completed. Diamond was used to compare the unigenes to the NCBI NR, KOG (eukaryotic ortholog groups), Gene Ontology (GO), Swiss-Prot, eggNOG, and Kyoto Encyclopedia of Genes and Genomes (KEGG) databases [34]. Functional analyses were conducted using the HMMER comparison of unigenes to the Pfam database [35]. The PlantTFDB database [36]was used to identify transcription factors (TFs).

Using Bowtie2 [37], the number of unigene reads in each sample was obtained. The expression of unigene Fragments Per Kilobase of transcript per Million Mapped reads (FPKM) was calculated using eXpress [38]. A principal components analysis (PCA) was performed using R (https://www.r-project.org/). The differentially expressed gene (DEG) screening threshold was set to $p < 0.05$ and |foldchange| > 2. The clusterProfiler package was used to perform GO and KEGG enrichment of the DEGs [39]. GOSemSim was used to calculate the similarity between GO terms [40]. GO term similarity clustering was conducted using ggtree [41]. Calculation results were selected if $q < 0.01$ in order to avoid the very general sets and limit the annotation of > 300 genes and GO terms of < 100 genes. According to the *p*-value screening, the top 10 KEGG pathways were used to map multiple sets of enriched analysis bubbles. Short Time-series Expression Miner (STEM) software was used to perform the trend cluster analysis [42], which was divided into 5 stages according to the time of occurrence; the combination of different stages of combined genes was input and normalized. The number of models was set to 50.

Screening for the top 5,000 genes of the leaf and root gene expression matrix (background gene set for all genes) was conducted according to the median absolute deviation (MAD) method. A matrix of the relationship between gene expression and sample traits was established using the weighted co-expression network analysis (WGCNA) package [43], which was subsequently transformed into a leader matrix to construct a joint analysis of the modules and traits.

Nine genes were selected to validate the transcriptome data using real-time quantitative PCR (RT-qPCR). SuperMix was removed and cDNA was synthesized using TransScript One-Step gDNA. The first strand of the cDNA fragment was synthesized from total RNA. RT-qPCR was performed on a real-time CFX96 Touch PCR instrument. The PCR reaction conditions were as follows: preheating at 95°C for 30 s, 40 cycles of heat denaturation at 95°C for 5 s, and annealing at 60°C for 34 s. The *T. fortunei* actin gene was used as the reference gene for data standardization. Each sample was repeated three times and the relative expression levels were calculated using the $2^{-\Delta\Delta Ct}$ method [44]. The primer sequences used in this study are provided (Table 1).

Abbreviations

ABA: abscisic acid

ACCase subunit alpha: acetyl-coenzyme A carboxylase carboxyl transferase subunit alpha, chloroplastic

AMC: the soil absolute moisture content

BP: Biological Process

CC: Cellular Component

cDNA: Complementary DNA

DEGs: differentially expressed genes

FPKM: Fragments Per Kilobase of transcript per Million Mapped reads

GO: Gene Ontology

KEGG: Kyoto Encyclopedia of Genes and Genomes

Lcha1-5: The light-harvesting complex I chlorophyll a/b binding protein 1-5

MAD: median absolute deviation

MDA: Malondialdehyde activity

MF: Molecular Function

PCA: principal components analysis

POD: Peroxidase

Pro：Proline

Re0.5d: Rehydration after 12 hours

Re1d: Rehydration after 1 day

Re3d: Rehydration after 3 days

Re6d: Rehydration after 6 days

ROS: reactive oxygen species

RT-qPCR: Real time quantitative PCR

Rv: root vitality

SAD: stearoyl-ACP desaturase

SOD: superoxide dismutase

STEM: Short Time-series Expression Miner

1. ***fortunei***: *Trachycarpus fortunei*

TF: transcription factors

WGCNA：Weighted correlation network analysis

Declarations

Ethics approval and consent to participate

Not applicable.

Consent for publication

Not applicable.

Availability of data and materials

The raw transcriptomic data generated during the current study are available from NCBI. All other data generated or analyzed during this study are included in this published article.

Competing interests

The authors declare that they have no competing interests.

Funding

The work was supported by Major Science and Technology Projects in Guizhou Province (Ministry of Science and Technology Major Project [2014] 6024). The funders did not play any roles in the design of the study, collection, analysis and interpretation of the relevant data, and writing the manuscript.

Author information

Affiliations

[1]College of forestry/[2]Institute for Forest Resources & Environment of Guizhou

[3]Key laboratory of forest cultivation in plateau mountain of Guizhou province, [4]Key laboratory of Plant Resource Conservation and Germplasm Innovation in M

Authors' contributions

X.F and Z.Y designed and executed the experiment; W.X.R conductedadditional analyses; X.F wrote the manuscript. All authors have read and approved the manuscript.

Corresponding author

Correspondence to Y. Zhao (zhy737@126.com)

Acknowledgments

We thank LetPub (www.letpub.com) for its linguistic assistance during the preparation of this manuscript.

References

1. Lan Z , Xiaoli W , Peng L , et al. Response of Trachycarpus fortunei Seedlings from Different Provenances to Drought Stress and Drought Resistance Evaluation[J]. Journal of Northeast Forestry University, 2017;(11), 1.
2. Hummel I, Pantin F, Sulpice R, et al. Arabidopsis plants acclimate to water deficit at low cost through changes of carbon usage: an integrated perspective using growth, metabolite, enzyme, and gene expression analysis[J]. Plant physiology, 2010;154(1): 357-372.
3. Showler A T. Water deficit stress-host plant nutrient accumulations and associations with phytophagous arthropods[J]. Abiotic stress-plant responses and applications in agriculture, 2013; 387-410.
4. Anjum S A, Xie X, Wang L, et al. Morphological, physiological and biochemical responses of plants to drought stress[J]. African Journal of Agricultural Research, 2011;6(9): 2026-2032.
5. Krasensky J, Jonak C. Drought, salt, and temperature stress-induced metabolic rearrangements and regulatory networks[J]. Journal of experimental botany, 2012; 63(4): 1593-1608.
6. Li H, Liu J, Zhang L, et al. Antioxidant responses and photosynthetic behaviors of Kappaphycus alvarezii and Kappaphycus striatum (Rhodophyta, Solieriaceae) during low temperature stress[J]. Botanical studies, 2016; 57(1): 21.
7. Contreras-Porcia L, Thomas D, Flores V, et al. Tolerance to oxidative stress induced by desiccation in Porphyra columbina (Bangiales, Rhodophyta)[J]. Journal of experimental botany, 2010; 62(6): 1815-1829.
8. Din J, Khan S U, Ali I, et al. Physiological and agronomic response of canola varieties to drought stress[J]. J Anim Plant Sci, 2011; 21(1): 78-82.
9. Sharma P, Jha A B, Dubey R S, et al. Reactive oxygen species, oxidative damage, and antioxidative defense mechanism in plants under stressful conditions[J]. Journal of botany, 2012; 2012.
10. Guo Y, Zhao S, Zhu C, et al. Identification of drought-responsive miRNAs and physiological characterization of tea plant (Camellia sinensis L.) under drought stress[J]. BMC plant biology, 2017; 17(1): 211.
11. Dalal V K, Tripathy B C. Water-stress induced downsizing of light-harvesting antenna complex protects developing rice seedlings from photo-oxidative damage[J]. Scientific reports, 2018; 8(1): 5955.
12. Luo F, Deng X, Liu Y, et al. Identification of phosphorylation proteins in response to water deficit during wheat flag leaf and grain development[J]. Botanical studies, 2018; 59(1): 28.
13. Michaletti A, Naghavi M R, Toorchi M, et al. Metabolomics and proteomics reveal drought-stress responses of leaf tissues from spring-wheat[J]. Scientific reports, 2018; 8(1): 5710.
14. Dace H, Sherwin H W, Illing N, et al. Use of metabolic inhibitors to elucidate mechanisms of recovery from desiccation stress in the resurrection plant Xerophyta humilis[J]. Plant Growth Regulation, 1998; 24(3): 171-177.
15. Collett H, Butowt R, Smith J, et al. Photosynthetic genes are differentially transcribed during the dehydration-rehydration cycle in the resurrection plant, Xerophyta humilis[J]. Journal of Experimental Botany, 2003; 54(392): 2593-2595.
16. Haas J C, Vergara A, Hurry V, et al. Candidate regulators and target genes of drought stress in needles and roots of Norway spruce[J]. bioRxiv, 2019; 517151.
17. Deeba F, Pandey A K, Pandey V. Organ specific proteomic dissection of Selaginella bryopteris undergoing dehydration and rehydration[J]. Frontiers in plant science, 2016; 7: 425.
18. Zhang K, Gan S S. An abscisic acid-AtNAP transcription factor-SAG113 protein phosphatase 2C regulatory chain for controlling dehydration in senescing Arabidopsis leaves[J]. Plant Physiology, 2012; 158(2): 961-969.
19. Rajasheker G, Jawahar G, Jalaja N, et al. Role and regulation of osmolytes and ABA interaction in salt and drought stress tolerance[M]//Plant Signaling Molecules. Woodhead Publishing, 2019; 417-436.
20. Wang K, He J, Zhao Y, et al. EAR1 negatively regulates ABA signaling by enhancing 2C protein phosphatase activity[J]. The Plant Cell, 2018; 30(4): 815-834.
21. Choi D W, Zhu B, Close T J. The barley (Hordeum vulgare L.) dehydrin multigene family: sequences, allele types, chromosome assignments, and expression characteristics of 11 Dhn genes of cv Dicktoo[J]. Theoretical and Applied Genetics, 1999; 98(8): 1234-1247.
22. Hand S C, Menze M A, Toner M, et al. LEA proteins during water stress: not just for plants anymore[J]. Annual review of physiology, 2011; 73: 115-134.
23. Li X, Liu Q, Feng H, et al. Dehydrin MtCAS31 promotes autophagic degradation under drought stress[J]. Autophagy, 2019; 1-16.
24. Ingram J, Bartels D. The molecular basis of dehydration tolerance in plants[J]. Annual review of plant biology, 1996; 47(1): 377-403

25. Li X, Zhang Q, Yang X, et al. OsANN3, a calcium-dependent lipid binding annexin is a positive regulator of ABA-dependent stress tolerance in rice[J]. Plant Science, 2019; 284: 212-220.
26. Rivas R, Falcão H M, Ribeiro R V, et al. Drought tolerance in cowpea species is driven by less sensitivity of leaf gas exchange to water deficit and rapid recovery of photosynthesis after rehydration[J]. South African Journal of Botany, 2016; 103: 101-107.
27. Challabathula D, Zhang Q, Bartels D. Protection of photosynthesis in desiccation-tolerant resurrection plants[J]. Journal of plant physiology, 2018; 227: 84-92.
28. Griffiths C A, Gaff D F, Neale A D. Drying without senescence in resurrection plants[J]. Frontiers in Plant Science, 2014; 5: 36.
29. John S P, Hasenstein K H. Biochemical responses of the desiccation-tolerant resurrection fern Pleopeltis polypodioides to dehydration and rehydration[J]. Journal of plant physiology, 2018; 228: 12-18.
30. Rajasekharan R, Nachiappan V. Fatty acid biosynthesis and regulation in plants[M]//Plant Developmental Biology-Biotechnological Perspectives. Springer, Berlin, Heidelberg, 2010; 105-115.
31. Liu Tingting. The Relationship Between Membrane Lipids Alteration and Drought Adaptation in Leaves of Maize Seedlings [D]. (2018) Chinese Academy of Sciences and Ministry of Education. (https://kns.cnki.net/KCMS/detail/detail.aspx?dbcode=CMFD&dbname=CMFD201802&filename=1018955651.nh&uid=WEEvREcwSlJHSldRa1FhcTdnTnhXM3ZPa1RBbCtlbVVzQmt3V0NqK21jST0=$9A
32. Xuekui, W. (2006). Plant physiology and biochemistry experiment principle and technology [M]. Beijjing.
33. Bolger A M, Lohse M, Usadel B. Trimmomatic: a flexible trimmer for Illumina sequence data[J]. Bioinformatics, 2014; 30(15): 2114-2120.
34. Buchfink B, Xie C, Huson D H. Fast and sensitive protein alignment using DIAMOND[J]. Nature methods, 2015; 12(1): 59.
35. Mistry J, Finn R D, Eddy S R, et al. Challenges in homology search: HMMER3 and convergent evolution of coiled-coil regions[J]. Nucleic acids research, 2013; 41(12): e121-e121.
36. Jin J, Zhang H, Kong L, et al. PlantTFDB 3.0: a portal for the functional and evolutionary study of plant transcription factors[J]. Nucleic acids research, 2013; 42(D1): D1182-D1187.
37. Langmead B, Salzberg S L. Fast gapped-read alignment with Bowtie 2[J]. Nature methods, 2012; 9(4): 357.
38. Roberts A. Ambiguous fragment assignment for high-throughput sequencing experiments[D]. UC Berkeley, 2013.
39. Yu G, Wang L G, Han Y, et al. clusterProfiler: an R package for comparing biological themes among gene clusters[J]. Omics: a journal of integrative biology, 2012; 16(5): 284-287.
40. Yu G, Li F, Qin Y, et al. GOSemSim: an R package for measuring semantic similarity among GO terms and gene products[J]. Bioinformatics, 2010; 26(7): 976-978.
41. Yu G, Smith D K, Zhu H, et al. ggtree: an R package for visualization and annotation of phylogenetic trees with their covariates and other associated data[J]. Methods in Ecology and Evolution, 2017; 8(1): 28-36.
42. Ernst J, Bar-Joseph Z. STEM: a tool for the analysis of short time series gene expression data[J]. BMC bioinformatics, 2006; 7(1): 191.
43. Langfelder P, Horvath S. WGCNA: an R package for weighted correlation network analysis[J]. BMC bioinformatics, 2008; 9(1): 559.
44. Schmittgen T D, Livak K J. Analyzing real-time PCR data by the comparative C T method[J]. Nature protocols, 2008; 3(6): 1101.

Table 1

Table 1. PCR primer sequences

No.	Gene_ID	Forward primer	Reverse primer	Product length(bp)	gene_name
	Reference Gene	5' TGAATCTGGTCCATCCATTGTC 3'	5' AGAACATACCATAACCAAGCTC 3'	60	Actin
1	TRINITY_DN53033_c0_g1_i1	5' ACCCTCCATCTCAGCCTTCA 3'	5' TGCCTCTGTGACCTCCTTTC 3'	146	accA
2	TRINITY_DN46177_c1_g1_i1	5' TGTCCCTATGTGCCTAGCAGTAA 3'	5' TCCGCATCCAACAATGTAAGAG 3'	76	Annexin D2
3	TRINITY_DN35842_c0_g1_i2	5' GACTGCTACTACGTCCCAACCTG 3'	5' CGACAAACCAATGGCTTCTTCA 3'	81	cytochrome P450
4	TRINITY_DN51483_c1_g1_i2	5' ATCAGGTCACCGTCCATAGC 3'	5' TTCTCCTTCAATCCCTTCTTTT 3'	169	Dehydrin COR410
5	TRINITY_DN52956_c0_g1_i2	5' ATAGGATTTGGCAGATAGCATTCG 3'	5' AACGCCTTCCATACCGCACT 3'	64	KCS-11
6	TRINITY_DN48903_c0_g2_i1	5' ACTTGCTAAGCCAGCCATTC 3'	5' AATCCCTTTGATGCCACTCC 3'	245	NAC 47
7	TRINITY_DN58051_c0_g2_i12	5' TGTGGCATCGTCTCAACT 3'	5' AATGAATGCACGGTTTGA 3'	87	P5CS
8	TRINITY_DN57760_c0_g1_i2	5' TGCTGGAAAGAGTTAGAAGAGG 3'	5' AGATTCGATATTATGGGTGGC 3'	62	PRODH
9	TRINITY_DN27793_c0_g1_i1	5' ATGGCAACCTTCCACTCTTCCTG 3'	5' ACCAACTGATCCGAGCACTCCTT 3'	116	YLS3

Figures

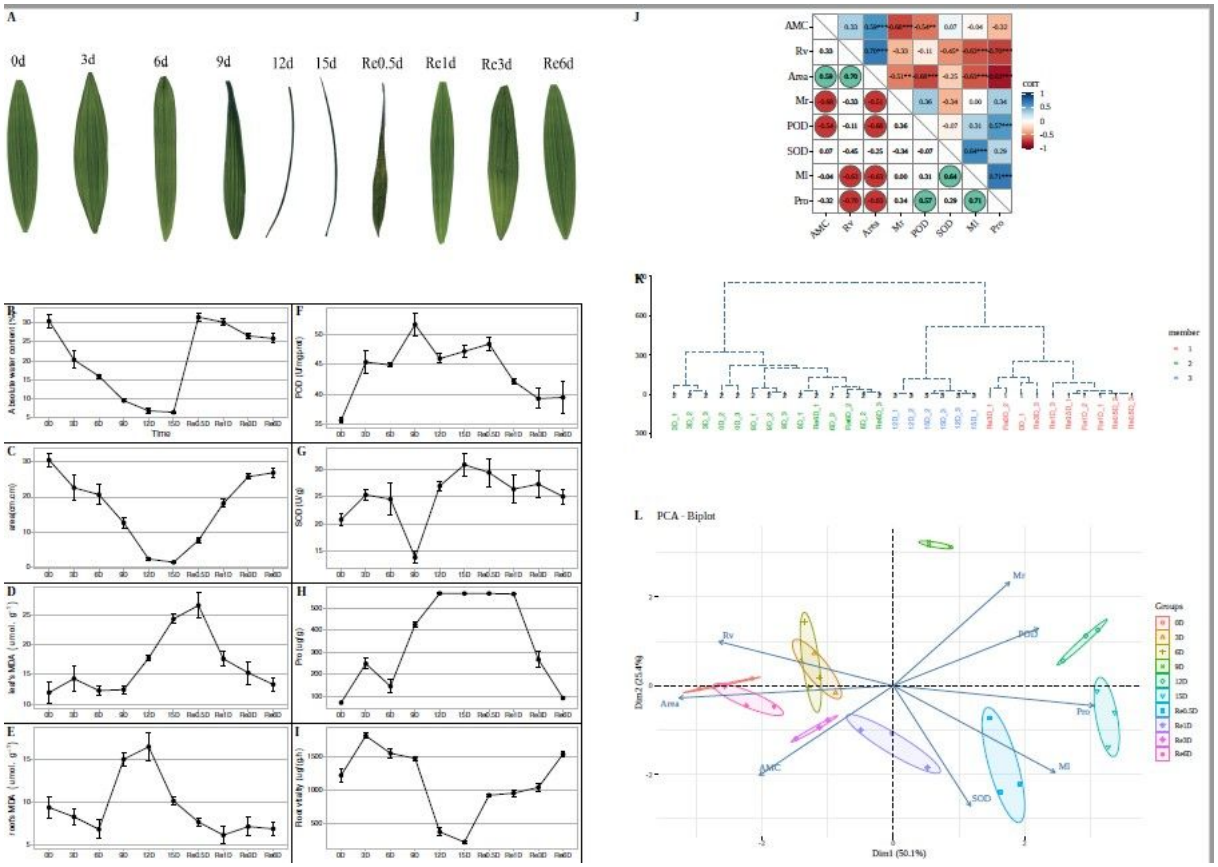

Figure 1

Changes in the physiological indicators of T. fortunei during drought stress and rehydration. A: Collection of T. fortunei leaf samples during the experiment; B: changes in the absolute moisture content of the soil; C: Changes in the area of T. fortunei leaves; D: changes in the MDA content of the leaves; E: changes in the MDA content of the roots; G: changes in the SOD activity of the leaves; H: changes in the Pro content of the leaves; I: changes in the root activity tetrazolium reduction intensity; J: correlation of the indices during stress; K: cluster analysis of the samples during stress; L:PCA of the physiological indexes during stress.

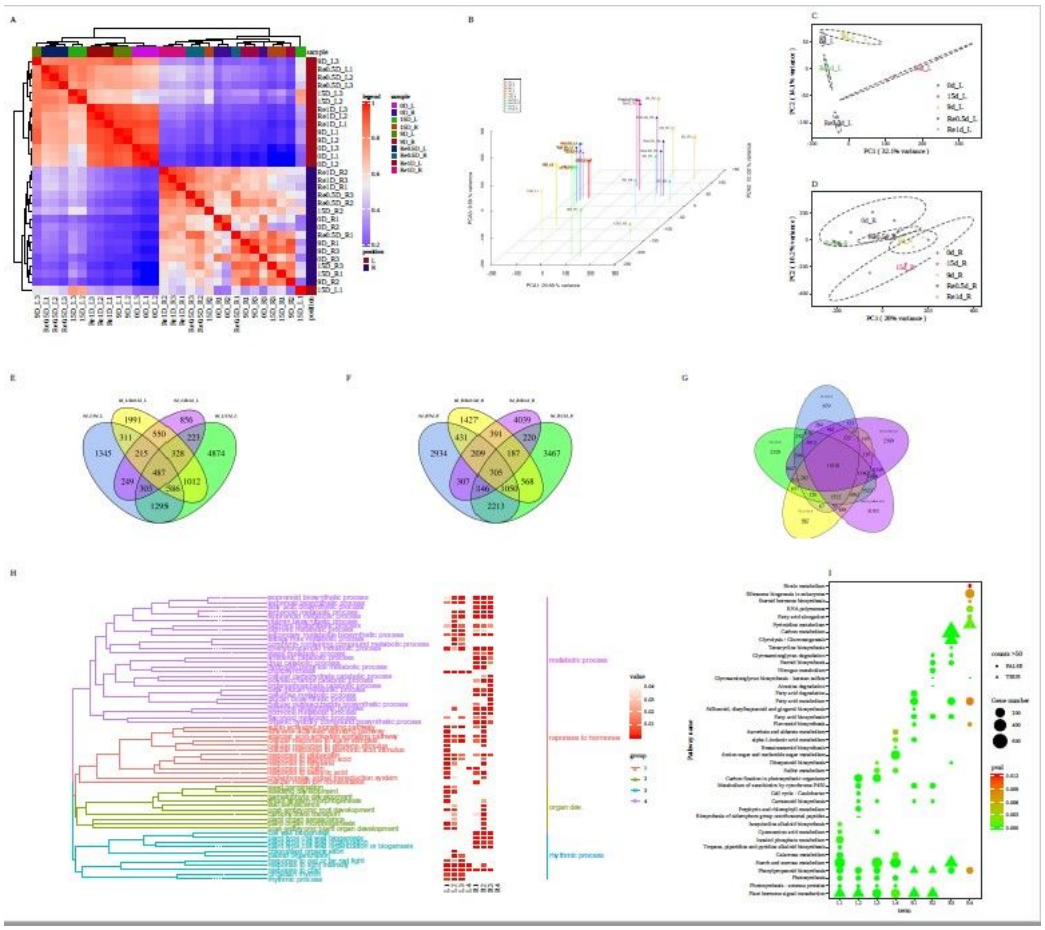

Figure 2

Analysis of transcriptome data and functional enrichment of differentially expressed genes A: Heatmap of the correlation of sample gene expression; B: three-dimensional PCA; C: Leaf PCA; D: Root PCA; E: Venn diagram of different leaf combinations; F: Venn diagram of different root combinations; G: Venn diagram of DEGs between the leaves and roots at different time periods; H: GO enrichment similarity clustering and heatmap; I: KEGG top 10 bubble chart. NOTE: L1 group = 0d_L/9d_L; L2 group = 0d_L/15d_L; L3 group = 0d_L/Re0.5d_L; L4 group = 0d_L/Re1d_L; R1 group = 0d_R/9d_R; R2 group = 0d_R/15d_R; R3 group = 0d_R/Re0.5d_R; R4 group = 0d_R/Re1d_R.

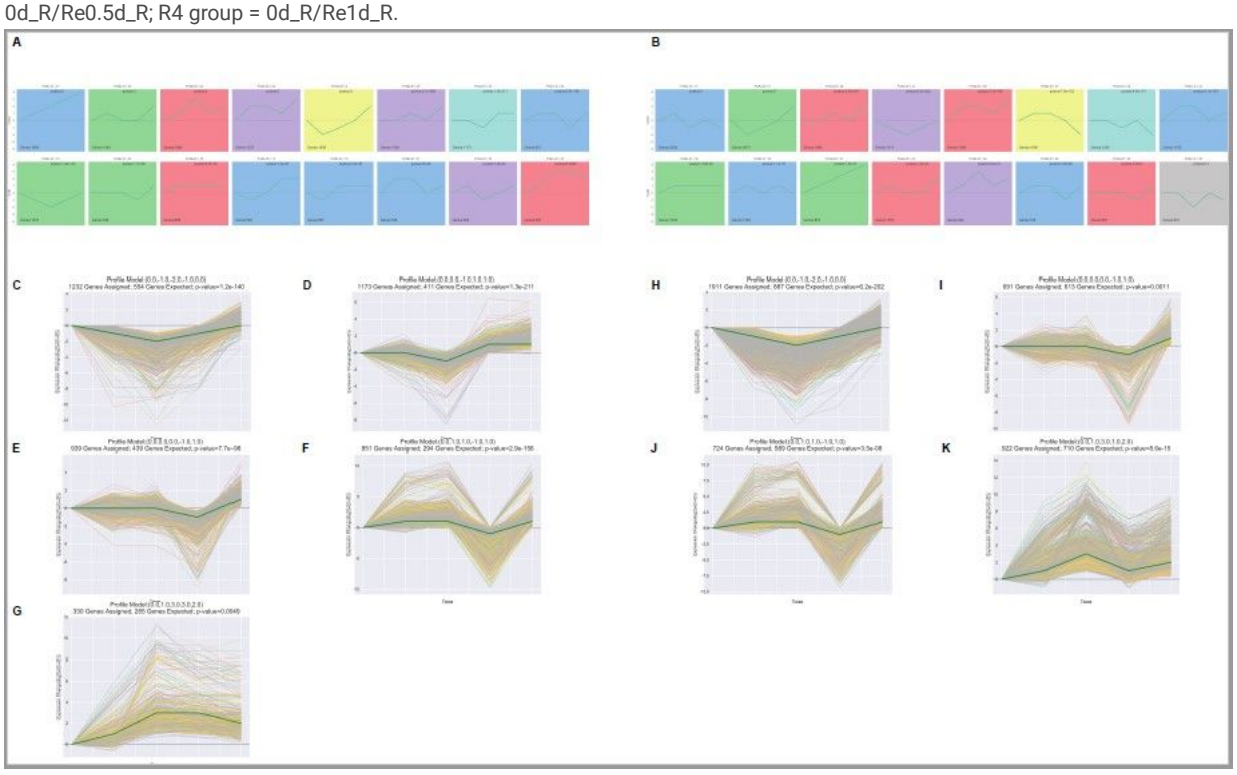

Figure 3

Cluster analysis of the gene expression trends during T. fortunei drought. A: Time-series analysis significance module of the leaves during drought stress; B: time-series analysis significance module of the roots during drought stress; C–G: selected significant leaf profiles (C: profile10, D: profile23, E: profile25, F: profile36, G: profile43); H–K: selected significant root profiles (H: profile10, I: profile25, J: profile36, K: profile42).

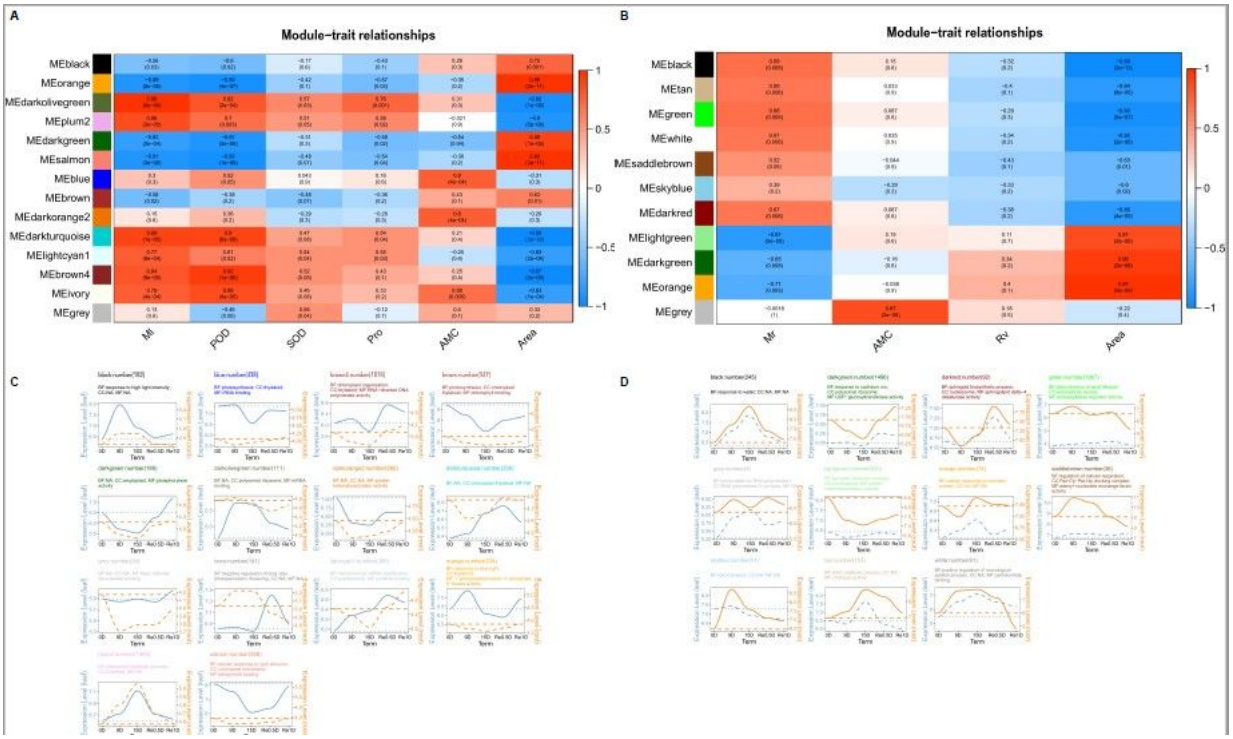

Figure 4

Analysis of the co-expression networks. A: Leaf trait and module correlation map; B: Root trait and module correlation map; C: Different module gene expression patterns in the leaves; D: Different module gene expression patterns in the roots. Note: C and D represent the expression trend of genes in the lower leaves and roots of different modules (the average of all genes in the module was normalized and linearly fitted); the left of the double axis is the tick mark ("# 6B9EC2") that represents the leaves; the right of the double axis is the tick mark ("# EE861A") that represents the roots; the text includes the number of gene modules, module names, and GO enrichment analysis results (displayed with the smallest p-value for each of BP, CC, and MF category).

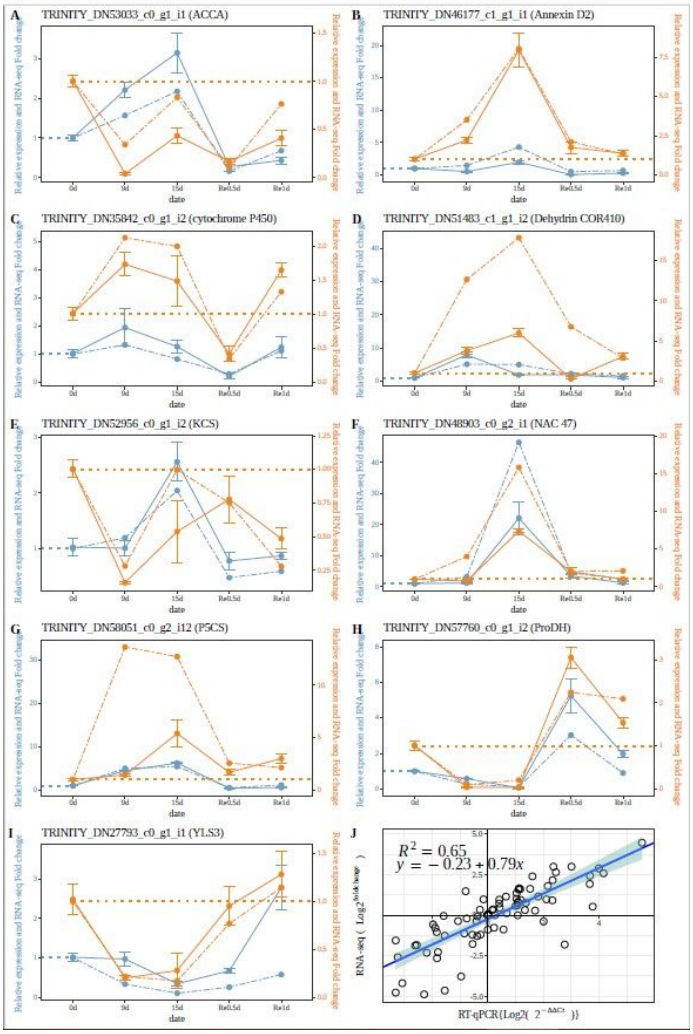

Figure 5

Correlation between the RT-qPCR and RNA-Seq data. Note: The left of the double axis is the tick mark ("# 6B9EC2") that represents the leaves; the right of the double axis is the tick mark ("# EE861A") that represents the roots; the solid line represents RT-qPCR; the dashed line represents the fold change.